The physics behind Van der Burgh's empirical equation, providing a new predictive equation for salinity intrusion in estuaries

Zhilin Zhang[1] and Hubert. H. G. Savenije[1]

[1]Department of Water Management, Faculty of Civil Engineering and Geosciences, Delft University of Technology, Delft, the Netherlands

Correspondence to: Zhilin Zhang (z.zhang-5@tudelft.nl)

Abstract.

The practical value of the surprisingly simple Van der Burgh equation to predict saline water intrusion in alluvial estuaries is well documented, but the physical foundation of the equation is still weak. In this paper we provide a connection between the empirical equation and the theoretical literature, leading to a theoretical range for Van der Burgh's coefficient of $1/2 < K < 2/3$
5   which falls within the feasible range of $0 < K < 1$. In addition, we developed a one-dimensional predictive equation for the dispersion of salinity as a function of local hydraulic parameters that can vary along the estuary axis, including mixing due to residual circulation. This type of mixing is relevant in the wider part of alluvial estuaries where preferential ebb and flood channels appear. Subsequently, this dispersion equation is combined with the salt balance equation to obtain a new predictive analytical equation for the longitudinal salinity distribution. Finally, the new equation was tested and applied to a large database
10   of observations in alluvial estuaries, whereby the calibrated K values appeared to correspond well with the theoretical range.

1 Introduction

Estuaries play an essential role in the human-earth system, affecting fresh water resources, the mixing between ocean and river water, and the health of aquatic ecosystems. This makes the functioning of estuarine systems an important field of research. A crucial element of estuarine dynamics is the interaction between saline and fresh water. The river discharges fresh water into
15   estuaries, flushing out the salt, while saline water penetrates landward as a result of density gradients. The temporal and spatial distribution of salinity in an estuary is determined by the competition between fresh water flushing and penetration of saline water by gravity.

Dispersion is the mathematical reflection of the spreading of a substance (e.g., salinity s) through a fluid as a function of a gradient in the concentration of the substance (e.g., the salinity gradient ds/dx). Hence, dispersion is the mathematical descrip-
20   tion of mixing. The physical process driving dispersion differs at different scales, depending on the dominant mechanism. For instance, at the molecular scale, the dominant mechanism is the Brownian movement of water molecules. At the scale of river flow, the process is driven by the transfer of friction from the riverbed into the cross section through turbulence. At this scale, the dispersion coefficient is called hydraulic eddy viscosity (K_E) (Dyer, 1997). The most important type of mixing in estuaries is the result of salinity gradients and the non-concurrence of the velocity and salinity field ($\overline{u's'}$) (MacCready, 2004), which is

the result of gravitational and tidal mixing processes. Finally, there is mixing by residual circulation, driven by the tide, where ebb and flood flows of different densities mix (e.g., Nguyen et al., 2008).

The dispersion resulting from density gradients is closely connected to the stratification number N_R, which is the balance between the potential energy resulting from the buoyancy of fresh water flowing into the estuary and the kinetic energy of the tide that provides the energy of mixing. This stratification number, also known as the Estuarine Richardson Number, is widely used in theoretical and practical studies (e.g., Fischer, 1972; Savenije, 1986; Kuijper and Van Rijn, 2011). If N_R is large, potential energy of river discharge dominates and stratification occurs; if N_R is small, the estuary is well mixed due to sufficient kinetic energy to reduce the density gradient.

Van der Burgh (1972) developed a purely empirical method with excellent practical performance (e.g., Savenije, 2005), combining into one equation the effects of all mixing mechanisms. However, the physical meaning of Van der Burgh's coefficient K is still unknown. Starting from this equation, the dispersion coefficient D can be shown to be proportional to the salinity gradient to the power of $K/(1-K)$ (Savenije, 2015). The literature presents different values for this power. Transferring these back with this relationship to Van der Burgh's coefficient, we found a theoretical value of 1/2 (Fischer, 1976; Thatcher and Najarian, 1983; Kuijper and Van Rijn, 2011), of 1 (Hansen and Rattray, 1965), a series of 0, 1/2 and 2/3 (Prandle, 1981; MacCready, 2004) or an empirical range of 0.20-0.75 (Gisen, 2015a). This article aims to provide a theoretical background for this coefficient.

Traditionally, researchers focused on vertical/longitudinal dispersion in prismatic estuaries (Hansen and Rattray, 1965) or cross-sectional varying estuaries (Prandle, 1981; MacCready, 2004). Fischer (1972) concluded that the lateral gravitational circulation is dominant over the sum of vertical oscillatory shear, net vertical circulation and lateral oscillatory shear. Lerczak and Geyer (2004) also stated the importance of lateral circulation to the momentum budget in estuaries but they used straight and prismatic channels, whereas the fact that the cross sections of natural alluvial estuaries obey an exponential function is relevant. In addition, almost all researchers split-up dispersion into its components by decomposed salinity and velocity (e.g., Hansen and Rattray, 1965; Fischer, 1972; Prandle, 1981; Thatcher and Najarian, 1983; MacCready, 2004, 2007, 2011; Lerczak and Geyer, 2004; Ralston and Stacey, 2005). Moreover, several researchers determined the dispersion based on a downstream boundary (Hansen and Rattray, 1965; Kuijper and Van Rijn, 2011; Gisen et al., 2015b), instead of calculating local dispersion on the basis of local hydraulic variables, as done in this research.

Although the processes of mixing and saline water intrusion are clearly complex and three-dimensional, it is remarkable that a very simple, empirical and one-dimensional approach, such as Van der Burgh's relationship, has yielded such surprisingly good results. This paper tries to bridge the gap between the theoretical approaches developed in the literature and the empirical results obtained with Van der Burgh's relationship, considering the complex interaction between tide, geometry, salinity and fresh water that govern dispersion in alluvial estuaries. In addition, we present a one-dimensional general dispersion equation for convergent estuaries that includes lateral exchange through preferential ebb and flood channels, using local tidal and geometrical parameters. This equation was validated on a broad database of salinity distributions in alluvial estuaries.

2 Linking Van der Burgh to the Traditional Literature

The one-dimensional mass-conservation equation averaged over the cross section over a tidal cycle can be written as (e.g., Savenije, 2005):

$$A\frac{\partial s}{\partial t} - |Q_f|\frac{\partial s}{\partial x} - \frac{\partial}{\partial x}\left(DA\frac{\partial s}{\partial x}\right) = 0 \tag{1}$$

where $A = Bh$ is the cross-sectional area, B is the width, h is the depth, s is the cross-sectional average salinity, t is time, Q_f is the fresh water discharge, x is the distance from estuary mouth and D is the effective longitudinal dispersion coefficient. The positive direction of flow is in the upstream direction.

At steady state, where $\partial s/\partial t = 0$, using the boundary condition: at $x \to \infty$, $s = s_f$ and $\partial s/\partial x = 0$, integration yields:

$$-\frac{|Q_f|}{A}(s - s_f) = D\frac{\mathrm{d}s}{\mathrm{d}x} \tag{2}$$

where s_f is the fresh water salinity, usually close to zero.

Van der Burgh (1972) found an empirical equation describing the tidal average longitudinal variation of the effective dispersion:

$$\frac{\mathrm{d}D}{\mathrm{d}x} = -K\frac{|Q_f|}{A} \tag{3}$$

where the dimensionless coefficient $K \in (0,1)$ according to Savenije (2005).

Combining equations (2) and (3) yields (Savenije, 1986, 1989, 1993a, b):

$$\frac{D}{D_1} = \left(\frac{s}{s_1}\right)^K \tag{4}$$

where D_1 and s_1 are the dispersion coefficient and salinity at a given point x_1, generally taken at the inflection point in the exponential estuary geometry. This equation is special in that it links the dispersion to the salinity, instead of the salinity gradient as most other researchers do (e.g., Fischer, 1976; Prandle, 1981; Thatcher and Najarian, 1983).

Interestingly, using equations (2) and (4) we can derive the dispersion as a function of the salinity gradient (Savenije, 2015):

$$\frac{D}{D_1} = \left(-\frac{AD_1}{|Q_f|s_1}\frac{\mathrm{d}s}{\mathrm{d}x}\right)^{\frac{K}{1-K}} \tag{5}$$

which connects the dispersion coefficient to local variables (A, $\mathrm{d}s/\mathrm{d}x$), boundary conditions (D_1, s_1), and K.

MacCready (2004, 2007) derived an equation for the exchange term theoretically:

$$\overline{u's'} - K_H\frac{\mathrm{d}s}{\mathrm{d}x} = \left(m_1\frac{h^2{u_f}^2}{K_S} + K_H\right)\left(-\frac{\mathrm{d}s}{\mathrm{d}x}\right) + m_2\frac{gc_sh^5u_f}{K_SK_E}\left(-\frac{\mathrm{d}s}{\mathrm{d}x}\right)^2 + m_3\frac{g^2{c_s}^2h^8}{K_S{K_E}^2}\left(-\frac{\mathrm{d}s}{\mathrm{d}x}\right)^3 = -D\frac{\mathrm{d}s}{\mathrm{d}x} \tag{6}$$

where $\overline{u's'}$ is the tidal average exchange flow salt flux, u' is the depth varying velocity, s' is the depth varying salinity, K_H is the along channel diffusion coefficient, $m_1 = \frac{2}{105}$, $m_2 = \frac{19}{420 \times 48}$ and $m_3 = \frac{19}{630 \times 48^2}$ are constant values following MacCready's

vertical integration, $u_f = |Q_f|/A$ is the depth-averaged velocity of fresh water, K_S is the effective vertical eddy diffusivity, g is the gravity acceleration, c_s is the saline expansivity equal to 7.7×10^{-4}, and K_E is the effective hydraulic eddy viscosity. For the latter, we use the equation $K_E = 0.1\frac{2}{\pi}u_*h$, with $u_* = \frac{\sqrt{g}}{C}\upsilon$ as the shear velocity in relation to the tidal velocity amplitude υ, where $C = K_m h^{1/6}$ is the coefficient of Chézy, and K_m is Manning's coefficient. Comparing the salt balance equation of Maccready to equation (2) implies that equation (6) is identical to $-D\frac{ds}{dx}$. MacCready assumed the estuary to be narrow and

5   rectangular, in the sense that cross-sectional shape does not basically modify the width-averaged dynamics. In the derivation, he also assumed the effective vertical eddy viscosity to be constant with depth, after Hansen and Rattray (1965), and that the salinity gradient of the depth-varying part is much smaller than the depth-averaged part, after Pritchard (1952). Additionally, other effects like salt storage, internal hydraulics and the Coriolis force were considered negligible.

   After division of all terms by the salinity gradient, it becomes an equation for the dispersion coefficient D:

10   $$D = \left(m_1 \frac{h^2 {u_f}^2}{K_S} + K_H\right) + m_2 \frac{gc_s h^5 u_f}{K_S K_E}\left(-\frac{ds}{dx}\right) + m_3 \frac{g^2 {c_s}^2 h^8}{K_S {K_E}^2}\left(-\frac{ds}{dx}\right)^2 \tag{7}$$

   whereby the first term is not dependent on the salinity gradient, the second is directly proportional to it, and the third term depends on the square of the salinity gradient.

   Based on equation (5) we can also derive an expression for the dispersion:

   $$D = D_1 \left(\frac{A_1 D_1}{l|Q_f|}\right)^{\frac{K}{1-K}}\left(-\frac{A}{A_1}\frac{l}{s_1}\frac{ds}{dx}\right)^{\frac{K}{1-K}} \tag{8}$$

15   where A_1 is the cross-sectional area at the inflection point (at $x = x_1$), $l = L - x_1$ is the distance from the inflection point to where salinity becomes the same as the fresh water salinity, L is the local intrusion length.

   Hence $D \propto \gamma^{\left(\frac{K}{1-K}\right)}$ with $\gamma = -\frac{A}{A_1}\frac{l}{s_1}\frac{ds}{dx}$. Given the function $F(\gamma) = \gamma^{\left(\frac{K}{1-K}\right)}$, a Taylor series expansion near $\gamma = 1$ can be derived as:

   $$F(\gamma) = \frac{(2K-1)(3K-2)}{2(1-K)^2} + \frac{K(2-3K)}{(1-K)^2}\left(\frac{A}{A_1}\frac{l}{s_1}\right)\left(-\frac{ds}{dx}\right) + \frac{K(2K-1)}{2(1-K)^2}\left(\frac{A}{A_1}\frac{l}{s_1}\right)^2\left(-\frac{ds}{dx}\right)^2 + R_2(x) \tag{9}$$

20   where $R_2(x)$ is the residual term, considered to be small. To analysis the importance of the different terms of (9), Figure 1 presents the factors $g_1 = \frac{(2K-1)(3K-2)}{2(1-K)^2}$, $g_2 = \frac{K(2-3K)}{(1-K)^2}$ and $g_3 = \frac{K(2K-1)}{2(1-K)^2}$. g_1 is the closure term which compensates for g_2 and g_3 so as to make $\sum g_i = 1$ $(i = 1, 2, 3)$. It is clear that the absolute value of the first term is much smaller than the density-driven terms. Also, the larger the value of K, the more important the third term is. This is in accordance with traditional literature if we analyze equation (9) mathematically. When $K = 1/2$, $F(\gamma) = \left(\frac{A}{A_1}\frac{l}{s_1}\right)\left(-\frac{ds}{dx}\right)$, dispersion is proportional to the

25   salinity gradient, meaning it driven by the longitudinal salinity gradient. If $K = 2/3$, $F(\gamma) = \left(\frac{A}{A_1}\frac{l}{s_1}\right)^2\left(-\frac{ds}{dx}\right)^2$ and dispersion is proportional to the square of the salinity gradient, which according to Fischer (1976) means that the dispersion is dominated by lateral exchange. According to these theoretical studies, K is in a range of 1/2 to 2/3, which is consistent with the situation where the dispersion combines longitudinal and lateral effects. The larger the value of K, the stronger the effect of lateral dispersion.

30   Considering only the density-driven terms in equations (7) and (9), the proportionality results in:

   $$\frac{2-3K}{2K-1} = 36\frac{K_E|Q_f|}{gc_s h^3 A_1}\frac{l}{s_1} = \frac{7.2E|Q_f|}{\sqrt{g}c_s h^2 A_1 CT}\frac{l}{s_1} = w \tag{10}$$

leading to an analytical expression for K:

$$K = \frac{2+w}{3+2w} \tag{11}$$

Since $w > 0$, the upper limit value of K is $2/3$ if the river discharge is small or the cross section is large and deep and w approaches zero. If the river discharge is large or the cross section is small and shallow, w is large and K converges to a value of $1/2$. We have used this expression to compute K values in real estuaries using the database of Savenije (2012). These K values are in a range of 0.51-0.64 (see Section 4.3).

Overall, there are three results for the estimation of Van der Burgh's coefficient: 1) from comparison with theoretical studies ($K = 1/2$ or $K = 2/3$), 2) by comparison between the salinity driven mixing terms ($1/2 < K < 2/3$), and 3) based on the empirical data set obtained by equation (11). These results are surprisingly close. In general, it can be concluded that the comparison between the theoretical work of MacCready and the analytical equations based on the Van der Burgh's relationship provides a solid foundation for the use of Van der Burgh's equation in one-dimensional analytical models.

3   Including Residual Circulation in Wide Estuaries

In the theory about mixing in estuaries, several authors have distinguished between tide-driven and density-driven dispersion (e.g., Hansen and Rattray, 1965; Banas et al., 2004). The tide is an active hydraulic driver that creates shear stresses in the flow as momentum, resulting from friction along the boundaries, transferred to the heart of the channel by turbulence. Generally these shear stresses reduce stratification and hence reduce dispersion. However, at large scale, the tide facilitates mixing by tidal trapping and residual circulation, which enhances dispersion. Tidal trapping results from irregularities of the channel, leading to pockets of relatively high or low salt concentrations that later reunite with the stream. The mixing length scale of tidal trapping is the tidal excursion. By using the tidal excursion as the mixing length, tidal trapping can be incorporated in a predictive equation. Residual circulation is more complicated. It can be a very powerful tide-driven mechanism in the wider parts of estuaries where the tide causes mixing by the cross-over of preferential ebb and flood channels that develop in wide estuaries, such as the Schelde, described by Nguyen et al. (2008). But how can we parameterize residual circulation? Here a different approach is followed from Nguyen et al. (2008), trying to combine this effect in the regular one-dimensional advection-dispersion equation.

3.1   Model Including Residual Circulation

Figure 2 presents the sketch of a box model used to include lateral exchange into longitudinal dispersion. Water particles in the middle can mix longitudinally and laterally within their respective mixing lengths. For the longitudinal mixing length we consider the tidal excursion and for the lateral exchange the half of estuary width. The balance of mass can then be described as:

$$\frac{V\Delta s_2}{\Delta t} = |Q_f|(s_2 - s_1) + d(s_1 - 2s_2 + s_3) + r(s_L - 2s_2 + s_R) \tag{12}$$

30 where $V = AE$ is the water volume, E is tidal excursion length, s is salinity, with subscripts of different locations, d and r are longitudinal and lateral exchange flows.

The balance equation then becomes:

$$V\frac{\partial s}{\partial t} - |Q_f|\frac{\partial s}{\partial x}\Delta x - d\frac{\partial^2 s}{\partial x^2}(\Delta x)^2 - r\frac{\partial^2 s}{\partial y^2}(\Delta y)^2 = 0 \tag{13}$$

where Δx and Δy are the mixing lengths, which are taken as $\Delta x = E$ and $\Delta y = B/2$.

5 The assumption used is that the lateral exchange is proportional to longitudinal (Fischer, 1972),

$$r\frac{\partial^2 s}{\partial y^2} \propto d\frac{\partial^2 s}{\partial x^2} \tag{14}$$

As a result, longitudinal and lateral processes can be combined into one single one-dimensional equation:

$$\frac{\partial s}{\partial t} - \frac{|Q_f|}{A}\frac{\partial s}{\partial x} - \frac{dE}{A}\left(1 + C_2\left(\frac{B}{E}\right)^2\right)\frac{\partial^2 s}{\partial x^2} = 0 \tag{15}$$

Comparing (15) with the traditional salt balance equation, the effective longitudinal dispersion is:

10 $$D = \frac{dE}{A}\left(1 + C_2\left(\frac{B}{E}\right)^2\right) \tag{16}$$

Subsequently, the longitudinal exchange flow d is assumed to be proportional to the amplitude of the tidal flow (driving the circulation) ($\widehat{Q_t} = A\upsilon$), and to the stratification number to the power of Van der Burgh's coefficient:

$$d = C_1(N_R)^K\widehat{Q_t} \tag{17}$$

with N_R defined as the ratio of potential energy of the river discharge to the kinetic energy of the tide over a tidal period:

15 $$N_R = \frac{\Delta\rho}{\rho}\frac{gh}{\upsilon^2}\frac{|Q_f|T}{AE} \tag{18}$$

where $\Delta\rho/\rho = c_s s$ is the relative density difference between river water and saline water and T is tidal period.

The reason why the exchange flow is a function of the stratification number to the power of K is because it is in agreement with equation (4), $\Delta\rho/\rho$ being directly proportional to s.

We then obtain a simple dimensionless expression for the dispersion coefficient, simulating to the one by Gisen et al. (2015b)
20 but incorporating lateral exchange flow:

$$\frac{D}{\upsilon E} = C_1(N_R)^K\left(1 + C_2\left(\frac{B}{E}\right)^2\right) \tag{19}$$

where C_1 and C_2 are constants .

3.2 Analytical Solution

In almost all estuaries, the ratio of width to excursion length is quite small, particularly upstream where salinity intrusion
25 happens. So for further analytical solutions we can focus on the first part of equation (19):

$$D = C_1(N_R)^K \upsilon E \tag{20}$$

The traditional approach by Savenije (2012) merely uses this equation as the boundary condition at $x = x_1$, after which $D(x)$ values are obtained by integration of the Van der Burgh's equation along the estuary axis. But, in principle, with this equation the dispersion can be calculated at any point along the estuary, provided local hydraulic and geometric variables are known. Using $\upsilon = \pi E / T$, equation (20) then becomes:

$$D(x) = C_1 (c_s g \pi)^K \left(\frac{s|Q_f|}{\upsilon^3 B} \right)^K \upsilon E \tag{21}$$

5   where all local variables are now function of x.

The following equations are used for the tidal velocity amplitude, width and tidal excursion:

$$\upsilon(x) = \upsilon_1 e^{\delta_\upsilon (x - x_1)} \tag{22}$$

$$B(x) = B_1 e^{\left(-\frac{x - x_1}{b} \right)} \tag{23}$$

10

$$E(x) = E_1 e^{\delta_H (x - x_1)} \tag{24}$$

where $\delta_\upsilon \approx \delta_H$ are damping/amplifying rate of tidal velocity amplitude and tidal range, b is the width convergence length (b_1 downstream of the inflection point and b_2 upstream).

At the inflection point, the predicted equation is given by:

15   $$D_1 = C_1 (c_s g \pi)^K \left(\frac{s_1 |Q_f|}{\upsilon_1^3 B_1} \right)^K \upsilon_1 E_1 \tag{25}$$

where the subscript '1' means parameters are evaluated at the inflection point ($x = x_1$).

Substitution of equations (22)-(25) in (21) gives:

$$D(x) = D_1 \left(\frac{s}{s_1} \right)^K e^{\Omega(x - x_1)} \tag{26}$$

with $\Omega = 2\delta_H - 3K\delta_H + K/b$.

20   Differentiating D with respect to x and using equation (26) results in:

$$\frac{\mathrm{d}D}{\mathrm{d}x} = K \frac{D}{s} \frac{\mathrm{d}s}{\mathrm{d}x} + \Omega D \tag{27}$$

Combining the result with the time-averaged salt balance, equation (27) results in:

$$\frac{\mathrm{d}D}{\mathrm{d}x} = \Omega D - K \frac{|Q_f|}{A} \tag{28}$$

For a prismatic channel ($b \to \infty$) with constant width and little tidal damping, $\Omega = 0$ and (28) becomes the Van der Burgh's

25   equation. As a result, the exponent of N_R in this model represents the Van der Burgh's coefficient.

Hydrology and
Earth System
Sciences

Discussions

The cross-sectional area A is given by:

$$A(x) = A_1 e^{\left(-\frac{x-x_1}{a}\right)} \tag{29}$$

where a is the cross-sectional convergence length (a_1 downstream of the inflection point and a_2 upstream).

Substitution of equation (29) in (28) gives:

$$\frac{dD}{dx} = \Omega D - K \frac{|Q_f|}{A_1} e^{\left(\frac{x-x_1}{a}\right)} \tag{30}$$

In analogy with Kuijper and Van Rijn (2011), the solution of this linear differential equation is:

$$\frac{D}{D_1} = \left[e^{\Omega(x-x_1)} + \frac{K|Q_f|}{A_1 D_1} \zeta \left(e^{\Omega(x-x_1)} - e^{(x-x_1)/a} \right) \right] \tag{31}$$

with $\zeta = \frac{a}{1-\Omega a}$.

The maximum salinity intrusion length is obtained from equation (31) after substitution of $D \to 0$ at $x = L$:

$$L = \zeta \ln \left(\frac{A_1 D_1}{K|Q_f|\zeta} + 1 \right) + x_1 \tag{32}$$

This is the same equation as in Savenije (2005) if $\zeta = a$.

Using equation (26), the longitudinal salt distribution becomes:

$$\frac{s}{s_1} = \left[1 + \frac{K|Q_f|}{A_1 D_1} \zeta \left(1 - e^{(x-x_1)/\zeta} \right) \right]^{1/K} \tag{33}$$

This solution is similar to the solution by Kuijper and Van Rijn (2011), with the difference that Kuijper and Van Rijn used a constant value of $K = 0.5$ and that their value of Ω depended on bottom slope.

So with these new analytical equations, the local dispersion and salinity can be obtained, using boundary condition at the inflection point. This method is limited since it only works when $B/E < 1$. If we want to account for residual circulation using equation (19), then we have to use numerical integration of equation (2) using (19) for D.

4 Empirical Validation

4.1 Summary Information

18 estuaries with quite different characteristics, covering a diversity of sizes, shapes and locations, have been selected from the database of Savenije (2012). It appears that all these alluvial estuaries can be schematized in one or two segments separated by a well-defined inflection point (Savenije, 2015). As an example, Figure 3 shows the geometry of two estuaries: Maputo with inflection point and Thames without inflection point. It can be seen that the natural geometry fits well on semilogarithmic paper, indicting an exponential variation of the cross section and width. Geometric data of all 18 estuaries are presented in Appendix A.

In Table 1 the general geometry of estuaries are summarized, where B_f is the bankfull stream width. It is obvious that these estuaries cover a wide range of sizes. Estuary with $x_1 = 0$ means there is no inflection point. In addition, the larger the a_2

(b_2), the slower the cross section (width) declines upstream. With a large b_2, a relatively small value of b_1 suggests the channel with a pronounced funnel shape with fast decrease of width near the mouth. In contrast, a relatively large value of b_2 indicates estuaries with near-prismatic shape. The same values of a and b indicate that the depth is constant.

Table 2 and 3 contain summary information of estuaries on different measurement dates, where H_1 is the tidal range at x_1, η is tidal amplitude, $\alpha = \frac{D_1}{|Q_f|}$ is the mixing coefficient and $\beta = \frac{Ka_2|Q_f|}{A_1 D_1}$ is the dispersion reduction ratio. Tidal excursion and

5   tidal period are more or less the same in all estuaries, except Lalang and Chao Phraya with a diurnal tide. Most estuaries damp upstream, with negative values of δ_H. In addition, most estuaries have a small tidal amplitude to depth ratio, which means relatively simple solutions of hydraulic equations are possible (Savenije, 2005). K values have been obtained by calibration of simulated salinities to observations in 18 estuaries. Using an automatic solver, the best result was obtained with $C_1 = 0.10$, $C_2 = 12$ and $K = 0.58$. For individual estuary, K values were obtained ranging between 0.45-0.78. In some estuaries $K > 2/3$,

10   which is because the empirical values only have the mathematically feasible limitation of $0 < K < 1$, and are not subject to the assumptions made in the theoretical derivation as by MacCready (2004). The dispersion at the inflection point has a range of 50-600 m^2/s in a diversity of estuaries which is consistent with Prandle (1981). The mixing coefficient demonstrates to what extent the dispersion overcomes the flushing by river flow. The larger the river discharge, the smaller the α, meaning it is difficult for the salinity to penetrate into the estuary. The dispersion reduction ratio determines the longitudinal variation of

15   dispersion. Fischer et al. (1979) suggested that the transition from a well-mixed to a strongly stratified estuary occurs when the values of stratification number N_R are in the range of 0.08-0.8. With a ratio of π between Fischer's and our expressions for the stratification number, the range becomes 0.25-2.51. It is obvious that all estuaries are partially- to well-mixed with N_R below 2.51.

4.2 Sensitivity to C_2

20   Through the use of C_2 we can use a single dispersion equation accounting for two-dimensional effects in a one-dimensional model. The assumption that lateral exchange is proportional to longitudinal dispersion suggests C_2 to be independent of x. Figure 4 and Appendix B demonstrate how salinity changes with varying C_2. Salinities were simulated by numerical solution of equation (2) with (19) based on the boundary condition at $x = x_1$. Typically, C_2 matters mainly near the mouth, but there is almost no effect on narrow estuaries like Lalang, Limpopo, Tha Chin and Chao Phraya. Hence, the inclusion of the residual

25   circulation improves the accuracy of salinity simulation in wide estuaries and more particularly near the mouth of the estuaries where the ratio of width to tidal excursion is relatively large.

To check the sensitivity to C_2, values of 1, 10 and 50 have been used to calculate salinity curves. It is demonstrated that the larger the value of C_2, the smaller the salinity gradient and the flatter the salinity curve near the estuary mouth. However, because of the interdependence of D, s and $\mathrm{d}s/\mathrm{d}x$ through equation (2) in the upstream part, a larger value of C_2 can lead to

30   larger salinities (e.g., Thames, Elbe, Edisto, Maputo and Corantijn). Basically, $C_2 = 10$ (green lines) can perform perfectly in 14 out of 18 estuaries (e.g., Maputo and Thames). We can see that larger values than $C_2 = 10$ cause exaggerated salinity in the downstream part of these estuaries which is why a general values of $C_2 = 10$ is recommended. The poorer results occur in estuaries that have peculiar shapes near the mouth. A larger value of C_2 applies to the Kurau. This may be because the

width is underestimated in the wide estuary mouth, due to misinterpretation of the direction of the streamline (The width is determined according to a line perpendicular to the streamline). As a matter of fact, the width should be larger and dispersion should be larger with smaller salinity gradients, which would then result in a lower value of C_2. The same applies to Endau. On the contrary, A smaller value of C_2 in Perak fits better, because of overestimating of the width. Here the topographical map suggests a wider estuary mouth, whereas the tidal flow is concentrated in a much narrower main channel due to a the north

5 bank protruding into the estuary and a spur from the south projecting into the mouth. The Selangor has a similar situation. It shows that the configuration of the mouth is important for the correct simulation of the salinity near the estuary mouth. But, fortunately, a relatively poor performance near the mouth of these estuaries does not affect the salinity distribution upstream as long as C_2 is not too large. In conclusion, $C_2 = 10$ appears to be a suitable default value as long as the trajectory of the tidal currents can be considered properly.

10 The poor fit in the downstream parts of the Lalang and Chao Phraya, in which measured salinities are lower than simulated, can be explained by a complex downstream boundary. The Lalang estuary has a pronounced riverine character and is a tributary to the complex estuary system of the Banyuasin, sharing its outfall with the large Musi river. So the salinity near its mouth is largely affected by the Musi. Also, pockets of fresh water can decrease the salinity near the confluence. The Chao Phraya opens to the Gulf of Thailand where the salinity is influenced by historical discharges rather than ocean salinity, remaining relatively

15 fresh. Other measurement uncertainties may cause outliers as well.

4.3   What Determines K

The physical meaning of the Van der Burgh's coefficient has been analyzed linking it to traditional theoretical research. Equation (10) shows a direct relation between this coefficient and MacCready's parameters which are measurable quantities. Hence, the coefficient is affected by tide, geometry and fresh water discharge. Gisen (2015a) assumed K to be independent on Q_f

20 and obtained a power function for predicting K, in which all parameters merely depended on the topography. Shaha and Cho (2011) also found K values to depend on river discharge and considered its value to increase upstream in a range of 0-1 due to different mechanisms along the estuary. Yet, from equation (10), the K value should be constant if the depth is constant along the estuary.

A 1:1 plot is presented in Figure 5, relating the empirical K values to the predicted values using equation (11). The predicted

25 K values have a smaller range (0.51-0.64) than the calibrated ones (0.45-0.78). However, they are quite similar considering they have been obtained from different approaches. This correspondence strengthens the physical basis of the Van der Burgh's equation. All K values are very close to 0.58 which may be a good starting value in estuaries where information on geometry and channel roughness is lacking.

5   Discussion and Conclusion

30 Overall, the single one-dimensional salinity intrusion model including residual circulation appears to work well in natural estuaries with a diversity of geometric and tidal characteristics, both by analytical and numerical computation. The new equation

is a simple and useful tool for analyzing local dispersion and salinity directly on the basis of local hydraulic variables. In a calibration mode, K is the only parameter to be calibrated using $C_1 = 0.10$ and $C_2 = 10$. In a predictive mode, a value of $K = 0.58$ can be used as a first estimate. If information on river discharge, roughness and geometry is available, K can be determined iteratively by taking $K = 0.58$ as the predictor and subsequently substituting s_1 and l from the first iteration by equations (10) and (11) and repeating the procedure until the process converges.

5   The addition of the factor $(1 + C_2(B/E)^2)$ in the dispersion equation proved valuable near the mouth of estuaries where residual circulation due to interacting ebb and flood channels dominate dispersion. The value $C_2 = 10$ was found to perform best in most estuaries, indicating that residual circulation is dominant in wide estuaries where ebb and flood currents prevail.

    Van der Burgh's coefficient determines the way dispersion relates to the stratification number by a power function. Two approaches, theoretical derivation from traditional literature and empirical validation based on observations in a large set of

10   estuaries, provided similar estimates of Van der Burgh's coefficient. Under MacCready's assumptions, there are three ways to estimate K: $0.51 < K < 0.64$ from empirical application of equations (10) and (11); $1/2 < K < 2/3$ as the physical boundaries of (11); and the comparison with traditional approximations ($K = 1/2$ or $K = 2/3$). After calibration of the new analytical model to the database of field observations, the values of K were in a range of 0.45-0.78 for a wide range of conditions, with an average of 0.58, close to the predicted values. MacCready's equation determines dispersion via a decomposition method, using

15   depth-varying velocity and salinity. Although these 1-D expressions of velocity and salinity may be simplifications of reality, the good correspondence between Van der Burgh's equation and MacCready's theory provides a strong theoretical basis for Van der Burgh's equation.

    A previous analytical salinity intrusion model was developed by Gisen (2015a), from which the K values resulted in a range of 0.20-0.75 by calibration and 0.22-0.71 by prediction. These solutions cover a wider range than our estimates because of

20   Gisen's assumption that K does not depend on river discharge and because of three improvements made in this paper. Firstly, we used the local hydraulic parameters to simulate the salinities, while Gisen used a constant depth and no damping ($\Omega = 0$). In addition, by using an uncertainty bound of 25 % on fresh water discharge we could reduce the inaccuracy of the tail of the salinity curve and obtain a better fit (where K matters most). And finally, all geometric analyses were improved by revisiting the fit to observations.

25   An important consequence of this research is that K depends on the water discharge. Where Gisen assumed K to be constant for each estuary, we find substantial variability for estuaries where a larger range of discharges is available: e.g. in the Maputo $0.57 < K < 0.70$; in the Limpopo $0.61 < K < 0.72$; and in the Edisto $0.48 < K < 0.58$. The implication of discharge dependence needs to be tested further for predictive purpose.

    In some particular cases, the simulated salinity with $C_2 = 10$ does not fit the observations near the estuary mouth. So one

30   should be aware of peculiar configurations of streamlines and geometries near the estuary mouth when using this model. MacCready and Geyer (2010) also pointed out that the effect of irregular channel shape is important. However, a poor fit near the estuary mouth has almost no effect on the total salinity intrusion length. It is suggested that in future research the assumption that lateral exchange is proportional to longitudinal exchange needs to be tested further. Finally, this predictive one-dimensional salinity intrusion model, having a stronger theoretical basis, may be a useful tool in ungauged estuaries.
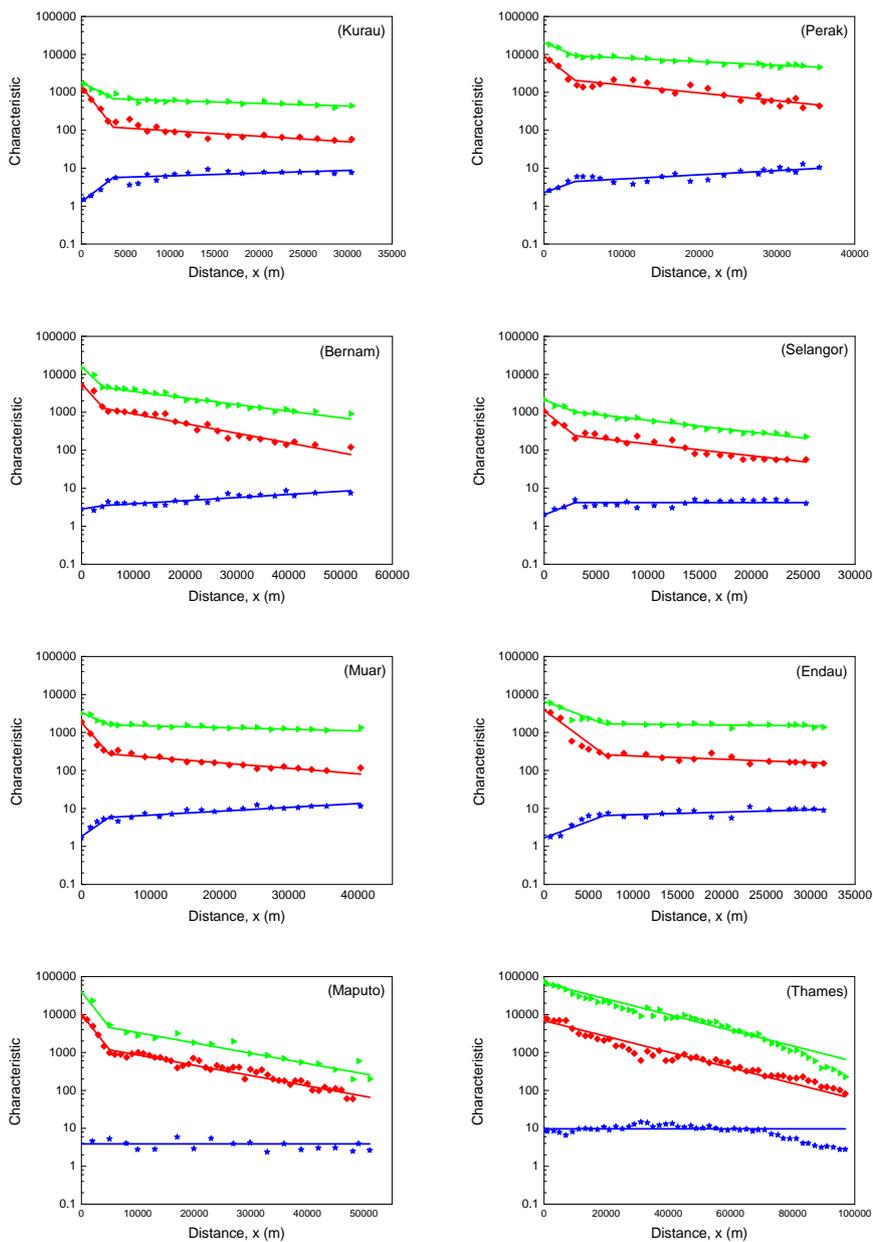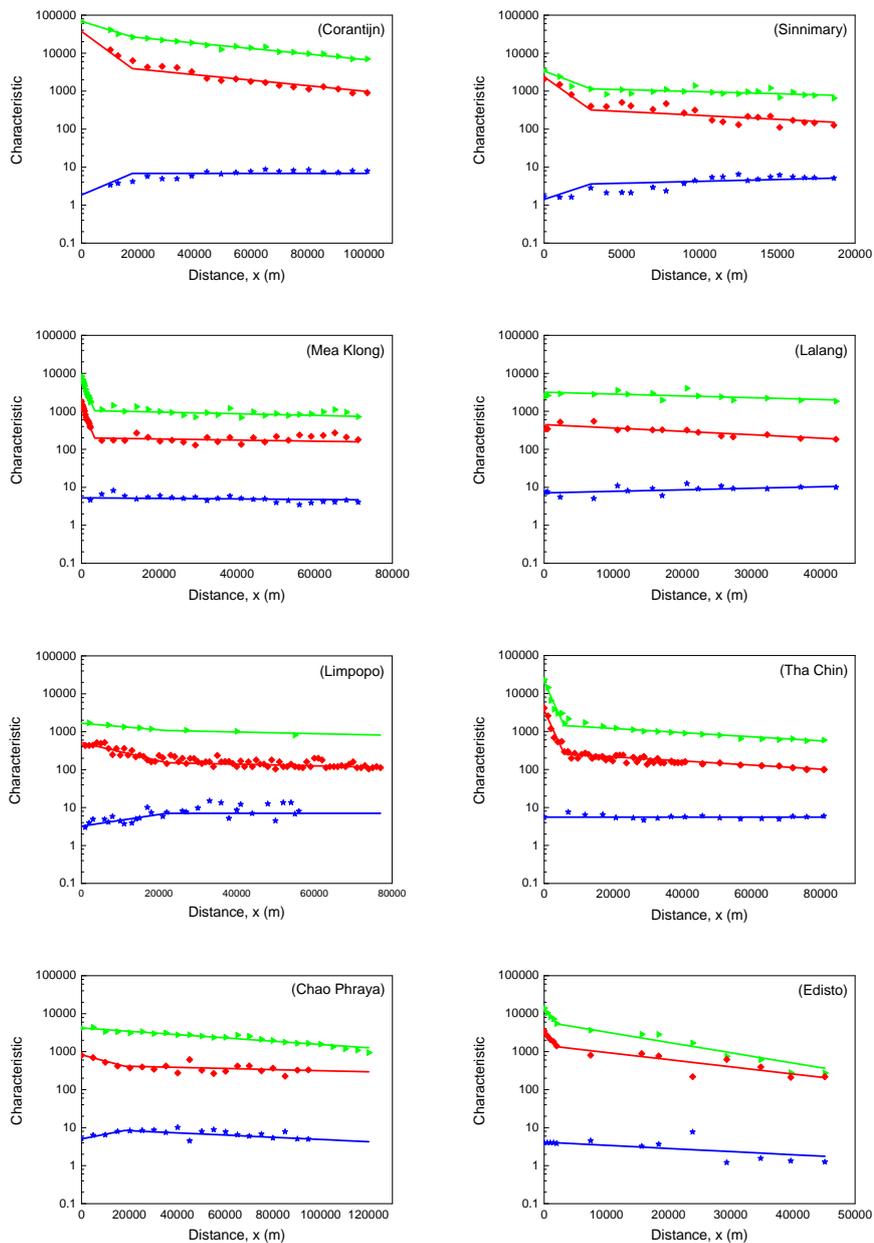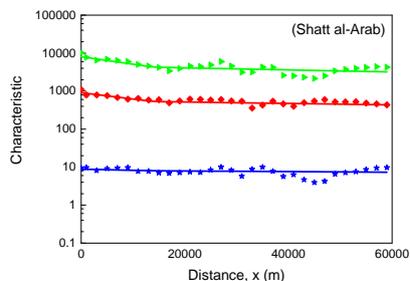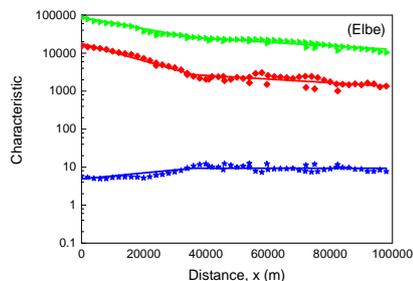
Appendix A: Notation

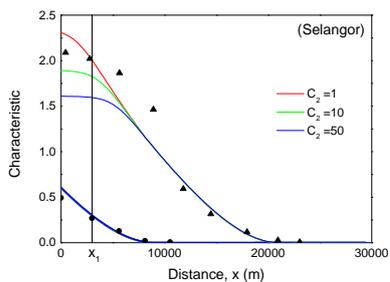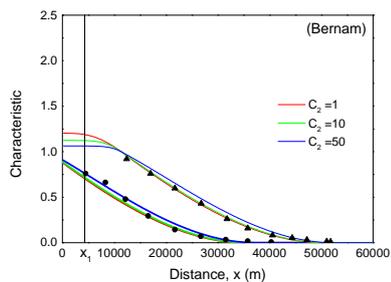| Symbol	Meaning	Dimension	Symbol	Meaning	Dimension
a	cross-sectional convergence length	[L]	Q_t	amplitude of tidal flow	[L^3/T]
A	cross-sectional area	[L^2]	r	lateral exchange flow	[L^3/T]
b	width convergence length	[L]	$R_2(x)$	residual term	[-]
B	width	[L]	s	salinity	[M/L^3]
B_f	bankfull stream width	[L]	s_f	fresh water salinity	[M/L^3]
C	coefficient of Chézy	[L$^{1/2}$/T]	s'	depth varying salinity	[M/L^3]
C_i	constant	[-]	t	time	[T]
c_s	saline expansivety	[-]	T	tidal period	[T]
d	longitudinal exchange flow	[L^3/T]	u	flow velocity	[L/T]
D	dispersion coefficient	[L^2/T]	u'	depth varying flow velocity	[L/T]
E	tidal excursion length	[L]	u_f	velocity of fresh water	[L/T]
g	gravity acceleration	[L/T^2]	u_*	shear velocity	[L/T]
g_i	factor	[-]	V	water volume	[L^3]
h	depth	[L]	x	distance	[L]
H	tidal range	[L]	α	mixing coefficient	[L^{-1}]
K	Van der Burgh's coefficient	[-]	β	dispersion reduction ratio	[-]
K_H	diffusion coefficient	[L^2/T]	γ	dimensionless argument	[-]
K_E	hydraulic eddy viscosity	[L^2/T]	δ	damping/amplifying rate	[L^{-1}]
K_m	Manning's coefficient	[L$^{1/3}$/T]	$\Delta x, \Delta y$	mixing lengths	[L]
K_S	vertical eddy diffusivity	[L^2/T]	υ	tidal velocity amplitude	[L/T]
l	intrusion length from inflection point	[L]	ζ	adjusted convergence length	[L]
L	intrusion length	[L]	η	tidal amplitude	[L]
m_i	constant	[-]	ρ	density of water	[ML^{-3}]
N_R	stratification number	[-]	Ω	adjustment parameter	[L^{-1}]
Q_f	fresh water discharge	[L^3/T]			

Hydrology and
Earth System
Sciences
Discussions

Open Access

EGU

Appendix B: Compilation of the geometry

Hydrology and
Earth System
Sciences

Open Access

EGU

Discussions

Appendix C: Sensitivity to C_2
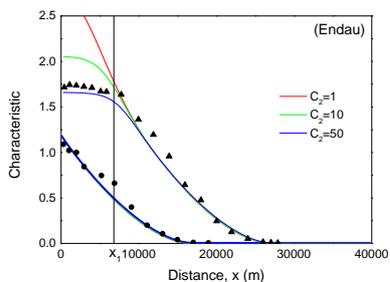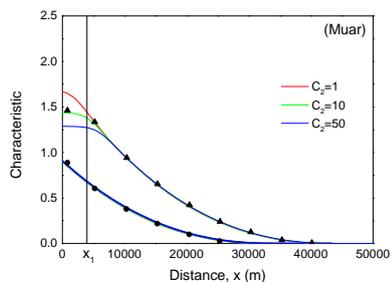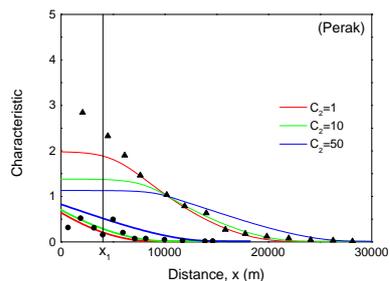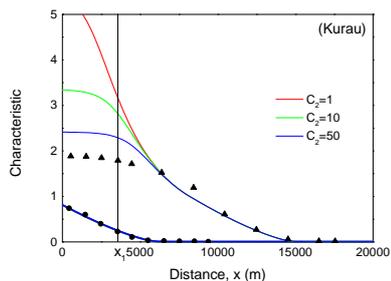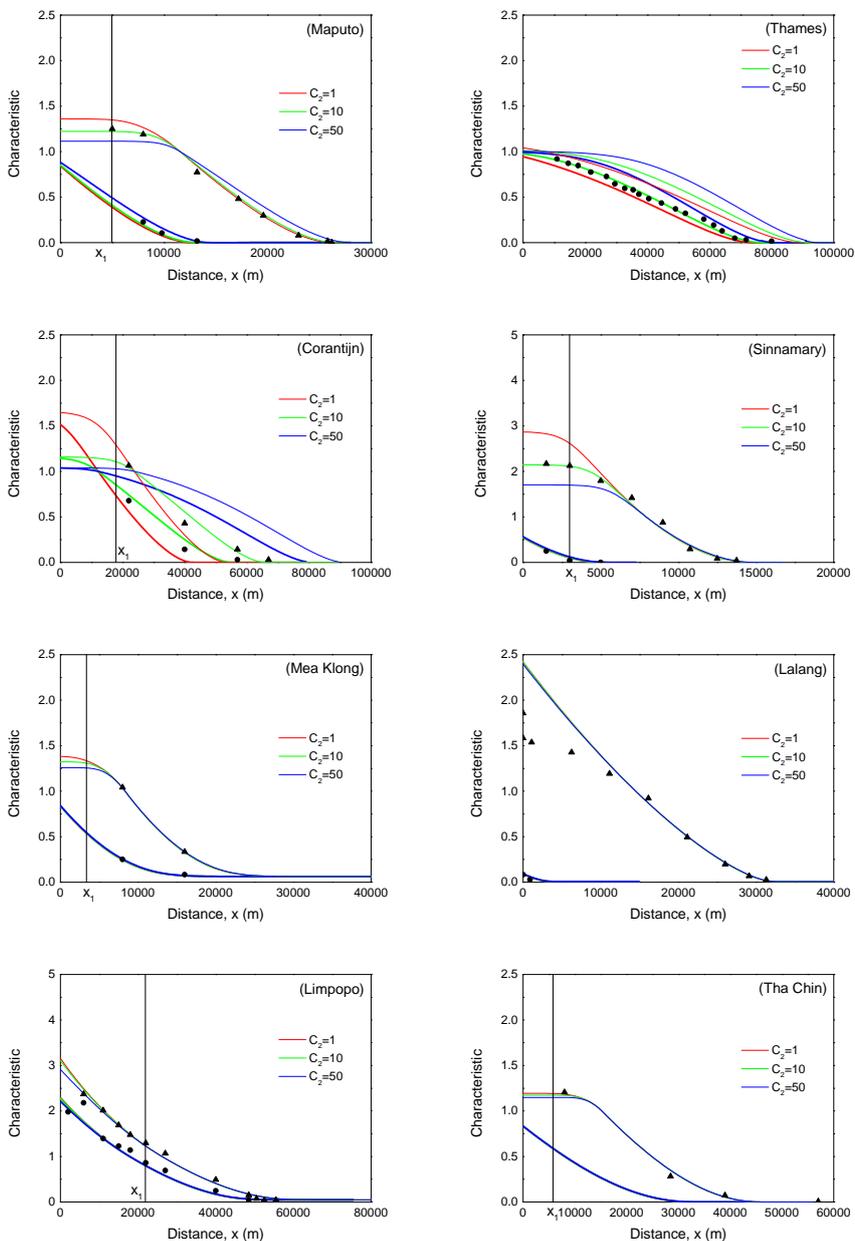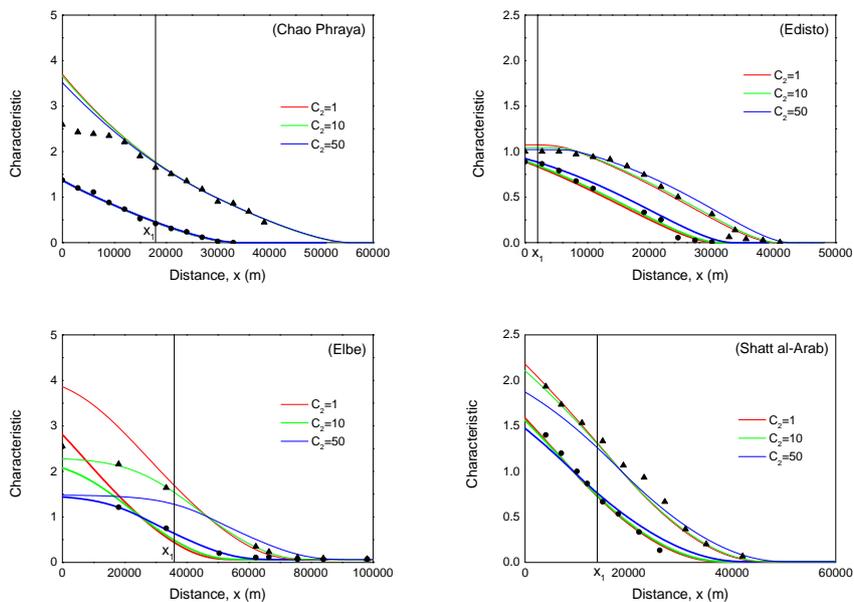
Hydrology and
Earth System
Sciences

Open Access

EGU

Discussions

References

Abdullah, A. D., Gisen, J. I. A., van der Zaag, P., Savenije, H. H. G., Karim, U. F. A., Masih, I., and Popescu, I.: Predicting the salt water intrusion in the Shatt al Arab estuary using an analytical approach, Hydrol. Earth Syst. Sci., 20, 4031–4042, 2016.

Banas, N. S., Hickey, B. M., and MacCready, P.: Dynamics of Willapa Bay, Washington: A highly unsteady, partially mixed estuary, J. Phys. Oceanogr., 34, 2413–2427, 2004.

Cai, H., Savenije, H. H. G., and Toffolon. M.: A new analytical framework for assessing the effect of sea-level rise and dredging on tidal damping in estuaries, J. Geophys. Res-Oceans, 117, C09023 doi:10.1029/2012JC008000, 2012.

Dyer, K. R.: (New revised issue) Estuaries: a Physical Introduction, John Wiley & Sons Aberdeen, UK, 1997.

Fischer, H. B.: Mass transport mechanisms in partially stratified estuaries, J. Fluid Mech., 53(4), 671–687, 1972.

Fischer, H. B.: Mixing and dispersion in estuaries, Annu. Rev. Fluid Mech., 8(1), 107–133, 1976.

Fischer, H. B., List, E. J., Koh. R. C. Y., Imberger., J., and Brooks., N. H.: Mixing in inland and coastal waters, Academic Press, New York, 1979.

Gisen, J. I. A.: Prediction in ungauged estuaries, Delft University of Technology, Delft, 2015a.

Gisen, J. I. A., Savenije, H. H. G., Nijzink., R. C., and Abd. Wahab., A. K.: Testing a 1-D analytical salt intrusion model and its predictive equations in Malaysian estuaries, Hydrolog. Sci. J., 60(1), 156–172, 2015b.

Hansen, D. V., and Rattray., M.: Gravitational circulation in straits and estuaries, J. Mar. Res., 23, 104–122, 1965.

Kuijper, K., and Van Rijn., L. C.: Analytical and numerical analysis of tides and salinities in estuaries; Part II: Salinity distributions in prismatic and convergent tidal channels, Ocean Dynam., 61(11), 1743–1765, 2011.

Lerczak, J. A., and Geyer., W. R.: Modeling the lateral circulation in straight, stratified estuaries, J. Phys. Oceanogr., 34(6), 1410–1428, 2004.

MacCready, P.: Toward a unified theory of tidally-averaged estuarine salinity structure, Estuaries, 27(4), 561–570, 2004.

MacCready, P.: Estuarine adjustment, J. Phys. Oceanogr., 37(4), 2133–2145, 2007.

MacCready, P., and Geyer, W. R.: Advances in estuarine physics, Annu. Rev. Mar. Sci., 2, 35–58, 2010.

MacCready, P.: Calculating estuarine exchange flow using isohaline coordinates, J. Phys. Oceanogr., 41, 1116–1124, 2011.

Nguyen, A. D., Savenije, H. H. G., Van der Vegen, M. and Roelvink, D.: New analytical equation for dispersion in estuaries with a distinct ebb-flood channel system, Estuar. Coast. Shelf S., 79(1), 7–16, 2008.

Prandle, D.: Salinity intrusion in estuaries, J. Phys. Oceanogr., 11(10), 1311–1324, 1981.

Pritchard, D. W.: Salinity distribution and circulation in the Chesapeake Bay Estuarine system, J. Mar. Res., 11(2), 106–123, 1952.

Ralston, D. K., and Stacey, M. T.: Longitudinal dispersion and lateral circulation in the intertidal Zone, J. Geophys. Res-Oceans, 110, C07015 doi:10.1029/2005JC002888, 1983.

Savenije, H. H. G.: A one-dimensional model for salinity intrusion in alluvial estuaries, J. Hydrol., 85(1-2), 87–109, 1986.

Savenije, H. H. G.: Salt intrusion model for high-water slack, low-water slack, and mean tide on spread sheet, J. Hydrol., 107(1-4), 9–18, 1989.

Savenije, H. H. G.: Composition and driving mechanisms of longitudinal tidal average salinity dispersion in estuaries, J. Hydrol., 144(1-4), 127–141, 1993a.

Savenije, H. H. G.: Determination of estuary parameters on basis of Lagrangian analysis, J. Hydraul.Eng-Asce, 119(5), 628–642, 1993b.

Savenije, H. H. G.: Salinity and tides in alluvial estuaries, Elsevier, New York, 2005.

Savenije, H. H. G.: Salinity and tides in alluvial estuaries, 2nd Edn, http://salinityandtides.com/, last access (19 Oct 2016), 2012.

Savenije, H. H. G.: Prediction in ungauged estuaries: An integrated theory, Water Resour. Res., 51(4), 2464–2476,2015.

Shaha, D. C., and Cho, Y.-K.: Determination of spatially varying Van der Burgh's coefficient from estuarine parameter to describe salt transport in an estuary, Hydrol. Earth Syst. Sci., 15, 1369–1377, 2011.

Thatcher, M. L., and Najarian, T.O.: Transient hydrodynamic and salinity simulations in the Chesapeake Bay Network, Estuaries, 6(4),

5   356–363, 1983.

Van der Burgh, P.: Ontwikkeling van een methode voor het voorspellen van zoutverdelingen in estuaria, kanalen en zeeen, Rijkswaterstaat Rapport, 10–72, 1972.
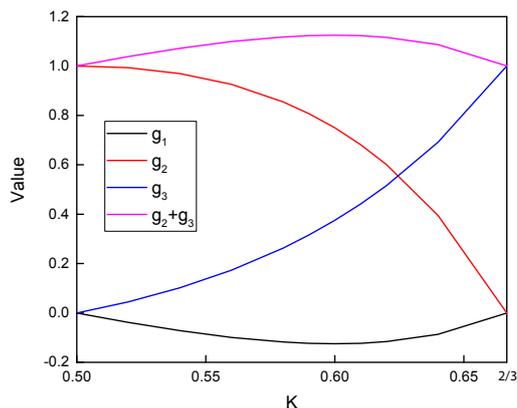
Hydrology and
Earth System
Sciences

Open Access

Discussions

EGU

Figure 1. Comparison between the factors in the Taylor series expansion of $F(\gamma)$ as a function of the Van der Burgh coefficient K.

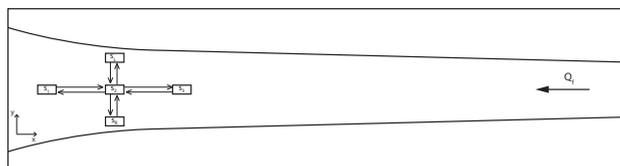**Figure 2.** Conceptual sketch for lateral and longitudinal mixing. Longitudinal and lateral mixing lengths are Δx and Δy, respectively.
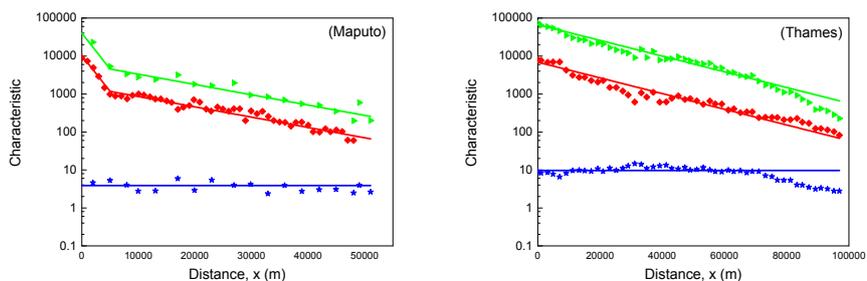

Figure 3. Semi-logarithmic presentation of estuary geometry, comparing simulated (lines) to the observations (symbols), including cross-sectional area (green), width (red) and depth (blue).
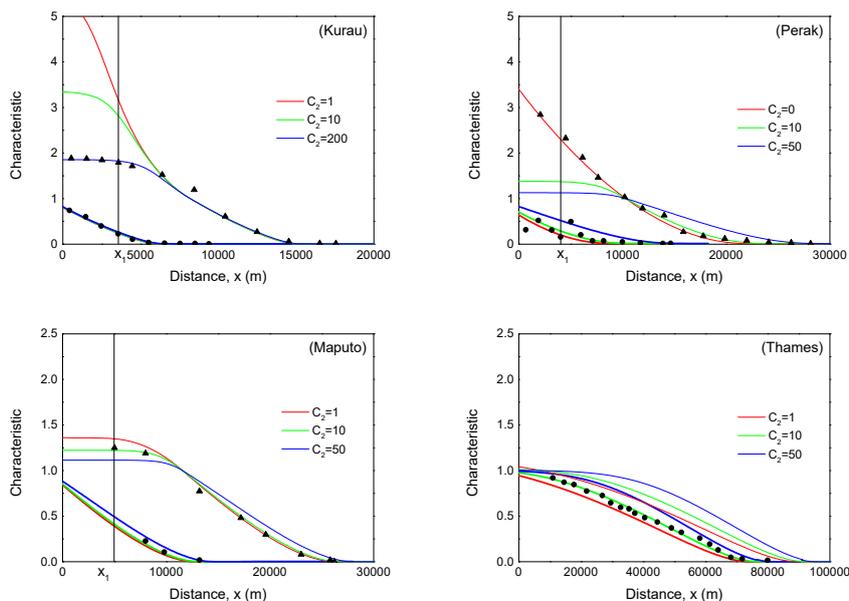
Hydrology and
Earth System
Sciences
Discussions

Figure 4. Comparison between simulated and observed salinity at high water slack (thin lines) and low water slack (thick lines), scaled by the salinity s_1 at the inflection point x_1 for different C_2 values. Observations at high water slack are represented by triangles and low water slack by circles. Observe that the Thames only has low water slack observations.
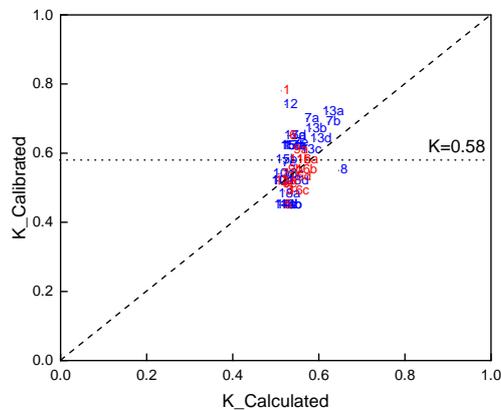

Figure 5. Comparison between predicted and calibrated K values. Labels are used to distinguish estuaries. The blue marks used K_m from Cai et al. (2012) and the red ones from Gisen (2015a).

Hydrology and
Earth System
Sciences

Open Access

Discussions

EGU

Table 1. Summary of the geometry of the estuaries

Label	Estuary	A_1 [m²]	a_1 [km]	a_2 [km]	b_1 [km]	b_2 [km]	x_1 [m]	h_1 [m]	B_f [m]	K_m [m$^{1/3}$s^{-1}]
1	Kurau	674	3.6	60	1.45	30	3600	5.6	20	30
2	Perak	9212	5	45	2.7	21	4000	4.5	130	65
3	Bernam	4460	3.4	25	2.9	17	4300	3.5	45	70
4	Selangor	1015	4	14	2	14	3000	4.2	35	40
5	Muar	1580	5.3	100	2.1	30	4000	5.8	55	45
6	Endau	1682	5	200	2.5	50	6800	6.5	72	45
7*	Maputo	4550	2.3	16	2.3	16	5000	3.9	100	70
8*	Thames	67000	21	21	21	21	0	9.7	50	51
9	Corantijn	26670	19	60	8	60	18000	6.8	400	40
10*	Sinnamary	1155	2.8	40	1.5	21	3000	3.6	95	50
11	Mae Klong	1038	1.8	200	1.8	300	3400	5.2	150	40
12*	Lalang	3184	90	90	49	49	0	7.1	130	70
13*	Limpopo	1075	50	200	18	200	22000	7.1	90	43
14*	Tha Chin	1430	2.2	80	2.2	80	5800	5.5	45	50
15*	Chao Phraya	3508	100	100	26	300	18000	8.5	200	51
16	Edisto	5401	2.1	16	2.1	23	2000	4.0	60	30
17*	Elbe	25472	29	90	19	90	36000	9.4	350	43
18*	Shatt al-Arab	4260	22	160	26	230	14000	8.0	250	38

Note (a): The estuaries with asterisk-marked label used K_m from Cai et al. (2012), while others from Gisen (2015a).

Note (b): Data about Shatt al-Arab Estuary comes from Abdullah et al. (2016).

Table 2. Summary of salinity measurement

Label	Date	s_1 [psu]	E_1 [m]	L [m]	T [s]	Q_f [m^3/s]	δ_H (10^{-6})[m^{-1}]	H_1 [m]	η/h [%]
1*	28-02-2013	15	9189	11000	44400	50	-6.3	2.8	25
2*	13-03-2013	8	12651	16000	44400	316	3	2.5	28
3*	21-06-2012	28	14103	42000	44400	42	1.7	3.5	50
4*	24-07-2012	14	12560	14000	44400	42	-3.7	4.0	47
5*	03-08-2012	18	10883	35000	44400	35	-2.68	2.0	17
6*	28-03-2013	17	10408	21000	44400	54	-1.3	1.9	14
7a	28-04-1982	29	13131	21000	44440	25	2	3.5	45
7b	15-07-1982	32	8080	30000	44440	8	2	2.1	27
7c*	19-04-1984	22	13131	20000	44440	120	2	3.3	43
7d	17-05-1984	24	13131	20000	44440	50	2	3.4	44
7e	29-05-1984	26	12626	23000	44440	40	2	3.0	39
8*	07-04-1949	31	14000	83000	44400	40	1.1	5.3	27
9a*	09-12-1978	14	11638	58000	44440	120	-1.7	1.8	13
9b	14-12-1978	12	12608	63000	44440	130	-1.7	2.2	16
9c	20-12-1978	10	12608	58000	44440	220	-1.7	1.6	11
10a	12-11-1993	9	8472	7600	44440	168	-5	2.6	36
10b	27-04-1994	7	10836	7800	44440	148	-5	2.9	40
10c*	03-11-1994	12	9851	9600	44440	112	-5	2.9	40
11a*	08-03-1977	24	9858	23000	44400	60	-4.2	1.5	14
11b	09-04-1977	25	7886	28000	44400	12	-4.2	2.1	20
12*	20-10-1989	14	29000	18000	86400	120	-0.54	2.6	18
13a	31-12-1982	24	7267	67000	44440	2	1.7	1.1	8
13b	14-07-1994	12	7267	47000	44440	5	1.7	1.0	7
13c*	24-07-1994	15	8305	58000	44440	5	1.7	0.93	7
13d	10-08-1994	17	8305	62000	44440	3	1.7	1.0	7
14a*	27-02-1986	21	18807	37000	44400	40	-10.6	2.4	22
14b	01-03-1986	25	13560	42000	86400	40	-5.5	1.8	17
14c	13-08-1987	17	11284	34000	44400	39	-10.6	1.9	17
15a*	05-06-1962	11	23068	43000	86400	63	-2.2	2.1	12

continued from previous page

Label	Date	s_1 [psu]	E_1 [m]	L [m]	T [s]	Q_f [m^3/s]	δ_H (10^{-6})[m^{-1}]	H_1 [m]	η/h [%]
15b	16-01-1987	1	13456	22000	86400	180	-2.2	2.4	14
15c	23-02-1983	8.5	18262	38000	86400	100	-2.2	1.5	9
15d	29-01-1983	12	24991	44000	86400	90	-2.2	1.5	9
16a*	12-07-2010	50	12773	35000	44400	15	-8.8	2.3	28
16b	13-07-2010	48	12773	38000	44400	14	-8.8	2.3	28
16c	14-07-2010	48	12282	37000	44400	25	-8.8	2.3	28
16d	15-07-2010	50	12282	35000	44400	25	-8.8	2.3	28
17a*	21-09-2004	10	21493	68000	44440	200	2	2.2	11
17b	21-09-2004	10.5	19344	69000	44440	200	2	3.2	17
18a	26-03-2014	11	9324	40000	44000	114	-5	1.6	10
18b	16-05-2014	15	9324	48000	44000	96	-5	2.3	15
18c	24-09-2014	27	14452	65000	44000	58	-5	2.2	14
18d*	05-01-2015	15	9324	42000	44000	63	-5	2.4	15

Note: The data chosen from each estuary with star-marked label is used for empirical calibration.

Table 3. Dispersion parameters using $C_2 = 10$

Label	K [-]	D_1 [m^2/s]	α [m^{-1}]	β [-]	N_R [-]	$K_{\text{calculated}}$ [-]
1	0.78	370	7.4	9.4	0.55	0.51
2	0.54	255	0.81	3.3	0.041	0.51
3	0.49	234	5.6	0.49	0.022	0.52
4	0.51	314	7.5	0.94	0.084	0.51
5	0.45	326	9.3	3.1	0.12	0.52
6	0.65	282	5.2	15	0.23	0.53
7a	0.70	80	3.2	0.77	0.019	0.57
7b	0.69	47	5.9	0.41	0.028	0.62
7c	0.57	281	2.3	0.86	0.068	0.52
7d	0.65	135	2.7	0.85	0.031	0.54
7e	0.63	133	3.3	0.67	0.030	0.55
8	0.55	239	6.0	0.030	0.0044	0.65
9a	0.61	178	1.5	0.92	0.018	0.55
9b	0.55	206	1.6	0.78	0.014	0.53
9c	0.51	292	1.3	0.86	0.019	0.52
10a	0.52	368	2.2	8.2	0.53	0.51
10b	0.52	335	2.3	8.0	0.17	0.51
10c	0.54	359	3.2	5.8	0.30	0.51
11a	0.52	484	8.1	12	0.51	0.51
11b	0.58	177	15	7.6	0.21	0.54
12	0.74	456	3.8	5.5	0.077	0.52
13a	0.72	46	23	5.8	0.056	0.62
13b	0.67	63	13	10	0.070	0.58
13c	0.61	86	17	6.6	0.059	0.57
13d	0.64	62	21	5.8	0.040	0.59
14a	0.45	536	13	1.9	0.033	0.51
14b	0.45	592	15	1.7	0.77	0.52
14c	0.45	376	9.6	2.6	0.12	0.51
15a	0.65	336	5.3	3.5	0.068	0.53

continued from previous page

Label	K	D_1	α	β	N_R	$K_{calculated}$
	[-]	[m^2/s]	[m^{-1}]	[-]	[-]	[-]
15b	0.58	163	0.90	18	0.089	0.51
15c	0.62	402	4.0	4.4	0.17	0.53
15d	0.62	485	5.4	3.3	0.083	0.52
16a	0.58	122	8.1	0.21	0.018	0.56
16b	0.55	130	9.3	0.18	0.016	0.56
16c	0.49	219	8.8	0.16	0.033	0.54
16d	0.53	195	7.8	0.20	0.034	0.54
17a	0.62	142	0.71	3.1	0.0050	0.53
17b	0.62	149	0.74	2.9	0.0073	0.53
18a	0.48	290	2.5	7.1	0.19	0.52
18b	0.45	324	3.4	5.0	0.22	0.52
18c	0.54	403	6.9	2.9	0.064	0.53
18d	0.52	234	3.7	5.2	0.14	0.54